Alberta Thy 14-04
UVIC–TH–04/08

Next-to-next-to-leading order calculations for heavy-to-light decays

Ian Blokland[1,2], Andrzej Czarnecki[1], Maciej Ślusarczyk[1,3], and Fyodor Tkachov[4]
1) Department of Physics, University of Alberta, Edmonton, AB T6G 2J1, Canada
2) Department of Physics and Astronomy, University of Victoria, Victoria, BC V8P 5C2, Canada
3) Institute of Physics, Jagiellonian University, Reymonta 4, 30-059 Kraków, Poland
4) Institute for Nuclear Research, Russian Academy of Sciences, Moscow, 117312, Russian Federation

We present technical aspects of next-to-next-to-leading order calculations for heavy-to-light decays such as top quark decay, semileptonic b quark decay into a u quark, muon decay, and radiative decays like $b \to s\gamma$. Algebraic reduction of integrals to a set of master integrals is described, methods of determining the master integrals are presented, and a complete list of master integrals is given. As a sample application, the top quark decay width is calculated to $\mathcal{O}\left(\alpha_s^2\right)$ accuracy.

PACS numbers: 12.38.Bx,14.65.Ha

I. INTRODUCTION

This paper describes the technical aspects of the calculation of $\mathcal{O}\left(\alpha_s^2\right)$ (next-to-next-to-leading order, or NNLO) heavy-to-light quark decays, such as $t \to bW$ and $b \to ul\nu$, that were presented in [1].

Computations in the NNLO for massive charged particle decays are challenging because of the presence of massive propagators which complicate loop and phase space diagrams. Here we focus on processes in which we have one gluon-radiating particle, Q, in the initial state, and one, q, in the final state, such as a semileptonic decay of a quark, $Q \to q + \text{leptons}$. Radiative decays like $b \to s\gamma$ and $b \to s + \text{leptons}$ also fall into this category. An analogous process with radiated gluons replaced by photons is the muon decay $\mu \to e\nu\bar{\nu}$.

A useful approach to such problems consists in expanding the decay amplitudes around some limit in which the diagrams can be computed analytically. In the past, all such expansions started with some point on the so-called zero-recoil line (see Fig. 1). Zero-recoil refers to the kinematic case in which the produced charged particle q remains at rest in the rest frame of the decaying Q.

In the present project we address the other kinematic extreme wherein a massive Q decays into two massless particles. One of the latter may be a pair of collinear massless leptons or a W boson in the limit of Q much heavier than the W. For a physical top quark decay, we can expand in m_W/m_t. Such an expansion, if taken to a sufficiently high order, also helps to describe the lepton invariant mass spectrum in the semileptonic $b \to u$ decay.

The main technical difficulty in constructing this expansion is the evaluation of a class of diagrams in which the four-momenta of all the final-state particles are on the order of the mass of the decaying quark. We explain here details of the methods we have used to overcome this obstacle.

This paper is organized as follows. In Section II we describe the calculational framework: the optical theorem, the various contributions needed to construct the expansion, and the ways of computing the necessary integrals. In Section III, we list the topologies of the Feynman integrals and give a set of so-called primitive or master integrals to which all others can be algebraically reduced. In Section IV, we present explicit examples of how typical primitive integrals can be evaluated. Section V contains our results and Section VI summarizes the paper. Throughout the presentation, we use top quark decay to illustrate the technical steps.

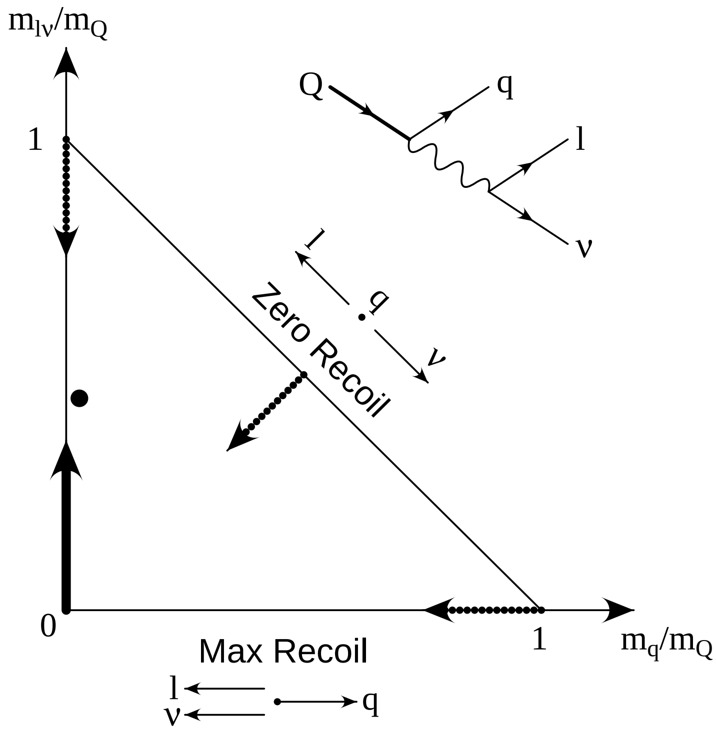

FIG. 1: Kinematic boundaries of the semileptonic decays $Q \to q +$ leptons. The solid arrow shows the expansion presented in this paper. Previously known expansions are indicated with dotted arrows [2, 3, 4]. Analytical results are now known along the whole zero-recoil line [5, 6] and at the lower left vertex of the triangle (this work). The dot at the left of the triangle indicates the kinematic configuration corresponding to the decay $t \to bW$.

II. CALCULATIONAL FRAMEWORK

A. Optical theorem

At $\mathcal{O}\left(\alpha_s^2\right)$, there are three classes of radiative corrections which contribute to the decay $t \to bW$: diagrams with virtual gluon loops, diagrams with real radiation, and diagrams with both a virtual gluon loop and a real gluon emission. The phase space calculations that would be required to calculate the decay rate in this approach are difficult even in the case that both masses m_b and m_W are neglected, and as we mentioned in the introduction, finding the functional dependence of the decay rate on m_W is one of our objectives. Our task becomes manageable by using the optical theorem to relate the decay width to the imaginary part of top quark self-energy diagrams:

$$\Gamma = \frac{\mathrm{Im}(\Sigma)}{m_t} \, . \tag{1}$$

The self-energy diagrams, Σ, that we must consider for the $\mathcal{O}\left(\alpha_s^2\right)$ decay rate are three-loop diagrams (two gluon loops and a $t \to bW \to t$ loop). The imaginary parts of these diagrams arise from the various cuts that can be made through the b, W, and g lines so that the two sides of the cut correspond to particular decay amplitudes. Despite the introduction of an additional loop, the calculation is feasible as a result of an assortment of techniques which have been developed to solve multiloop integrals analytically with the help of symbolic computation software.

B. Asymptotic expansions

With $m_b = 0$, there are two scales in the problem: m_t and m_W. We define an expansion parameter $\omega = m_W^2/m_t^2$ so that the two scales can be expressed as hard and soft ($\mathcal{O}(1)$ and $\mathcal{O}(\sqrt{\omega})$, respectively) using m_t as the unit of energy. The asymptotic expansion in powers and logarithms of ω of the contributing integrals is performed using the method of asymptotic operation [7], and contributions associated with the two scales are identified using the following heuristic mnemonic. The loop momenta flowing through the gluon lines must be hard or else scaleless integrals (which vanish in dimensional regularization) will arise. This leaves us with two regions to consider, depending on the scale of the loop momentum flowing through the W line. In the first region, all the loop momenta are hard and the Euclidean-space W propagator can be expanded as a series of massless propagators:

$$\frac{1}{k^2+m_W^2} = \frac{1}{k^2} - \frac{m_W^2}{k^4} + \frac{m_W^4}{k^6} - \frac{m_W^6}{k^8} + \dots \, . \tag{2}$$

After the integration, powers of m_W^2/k^2 will become powers of ω.

In the second region, the gluon momenta are hard but the loop momentum flowing through the W is soft. As a result, this loop momentum (k) decouples from the other momenta (ℓ) flowing through the b quark lines via the expansion

$$\frac{1}{(k+\ell)^2} = \frac{1}{\ell^2} - \frac{(k^2+2k\ell)}{\ell^4} + \frac{(k^2+2k\ell)^2}{\ell^6} - \frac{(k^2+2k\ell)^3}{\ell^8} + \dots \, . \tag{3}$$

Consequently, the diagrams in this region factor into a product of a two-loop self-energy-type integral and a one-loop vacuum bubble integral with a scale of m_W. The leading contribution from this second region is $\mathcal{O}\left(\omega^2\right)$; the interplay between the two regions gives rise to terms with a formally large logarithm $\ln \omega$.

C. Single-scale integrals

With the asymptotic expansions in place to extract the functional dependence of the top decay width on m_W, we have reduced the problem to that of solving single-scale self-energy loop integrals. The indispensable tools for doing this are integration-by-parts identities, used to reduce loop integrals with arbitrary powers of denominator factors to a small set of master integrals [8]. There are two approaches with which these identities can be applied to a collection of loop integrals. In the traditional method, one inspects the structure of the identities and rearranges them manually into the form of recurrence relations for a complete solution of the system. This method has proven to be very successful in numerous applications (e.g., [4, 9, 10, 11, 12, 13]) but it requires much human work to implement.

Recently, Laporta [14] succeeded in developing a targeted solution of the linear system (for only those integrals that are needed in a given problem) [15]. This was not previously practical as it is much more expensive computationally. In our calculation we used the traditional complete approach (programmed in FORM [16]) as well as a modified version of the new targeted algorithm for which we implemented a dedicated computer algebra program. In both cases we independently obtained identical results. This serves as a check of correctness and also enables us to compare the two methods [17].

III. LIST OF TOPOLOGIES AND MASTER INTEGRALS

In the "soft" loop-momentum region, the diagrams factor into a product of a two-loop self-energy-type integrals and a one-loop vacuum bubble integral with a scale of m_W. The bubble integral is purely real and can be solved easily. The entire set of two-loop self-energy integrals was first solved in [18]; the contributions from this region are therefore quite straightforward.

In the "hard" loop-momentum region, we need to extract the imaginary parts of genuine three-loop integrals. We identify 9 master topologies in terms of which all 36 $\mathcal{O}\left(\alpha_s^2\right)$ diagrams can be expressed. The diagrams which give rise to these master topologies are shown in Fig. 2. They are labeled by the letters A through I in analogy with the notation of [19] for the $\mathcal{O}\left(\alpha^2\right)$ contributions to muon decay. We use dimensional regularization ($D \equiv 4-2\epsilon$) and take the top quark mass as the unit of energy, $m_t \equiv 1$. Using the notation $[d^Dk] = d^Dk/(2\pi)^D$ we define the following Euclidean-space loop integrals (p is the incoming momentum),

$$\begin{aligned} A(a_1,a_2,a_3,a_4,a_5,a_6,a_7,a_8,a_9) &= \int \frac{[d^Dk_1][d^Dk_2][d^Dk_3]}{k_1^{2a_1}(k_1+p)^{2a_2}(k_1+k_3+p)^{2a_3}(k_1+k_2+k_3+p)^{2a_4}} \\ &\quad \times \frac{1}{[(k_2+k_3+p)^2+1]^{a_5}(k_3^2+2k_3p)^{a_6}k_2^{2a_7}k_3^{2a_8}(2k_2p)^{a_9}} \\ B(a_1,a_2,a_3,a_4,a_5,a_6,a_7,a_8,a_9) &= \int \frac{[d^Dk_1][d^Dk_2][d^Dk_3]}{k_1^{2a_1}(k_1+p)^{2a_2}(k_1+k_2+p)^{2a_3}(k_1+k_2+k_3+p)^{2a_4}} \end{aligned} \tag{4}$$

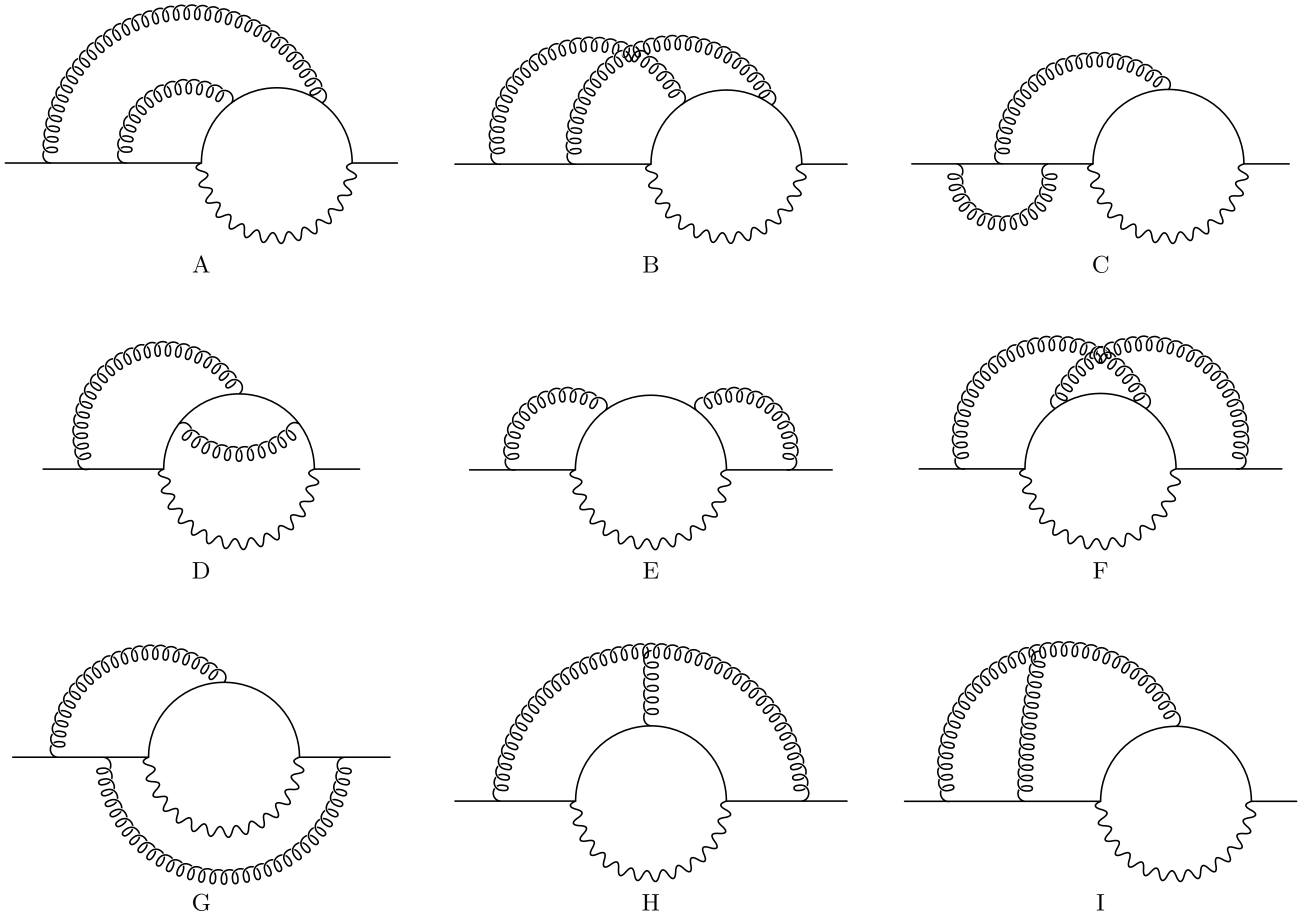

FIG. 2: The nine $\mathcal{O}(\alpha_s^2)$ diagrams for $t \to bW$ which constitute the master three-loop topologies of the calculation.

$$\times \frac{1}{[(k_2+k_3+p)^2+1]^{a_5}(k_3^2+2k_3p)^{a_6}k_2^{2a_7}k_3^{2a_8}(2k_2p)^{a_9}} \tag{5}$$

$$C(a_1,a_2,a_3,a_4,a_5,a_6,a_7,a_8,a_9) = \int \frac{[d^Dk_1][d^Dk_2][d^Dk_3]}{k_1^{2a_1}(k_1+p)^{2a_2}(k_1+k_2+p)^{2a_3}k_2^{2a_4}(k_2^2+2k_2p)^{a_5}}$$
$$\times \frac{1}{[(k_2+k_3+p)^2+1]^{a_6}(k_3^2+2k_3p)^{a_7}k_3^{2a_8}(2k_1k_3)^{a_9}} \tag{6}$$

$$D(a_1,a_2,a_3,a_4,a_5,a_6,a_7,a_8,a_9) = \int \frac{[d^Dk_1][d^Dk_2][d^Dk_3]}{k_1^{2a_1}(k_1+p)^{2a_2}(k_1+k_2+p)^{2a_3}(k_1+k_2+k_3+p)^{2a_4}}$$
$$\times \frac{1}{(k_1+k_3+p)^{2a_5}k_2^{2a_6}k_3^{2a_7}(k_3^2+2k_3p)^{a_8}(2k_2p)^{a_9}} \tag{7}$$

$$E(a_1,a_2,a_3,a_4,a_5,a_6,a_7,a_8,a_9) = \int \frac{[d^Dk_1][d^Dk_2][d^Dk_3]}{k_1^{2a_1}(k_1+p)^{2a_2}(k_1+k_2+p)^{2a_3}(k_1+k_3+p)^{2a_4}k_2^{2a_5}}$$
$$\times \frac{1}{k_3^{2a_6}(k_2^2+2k_2p)^{a_7}(k_3^2+2k_3p)^{a_8}(2k_2k_3)^{a_9}} \tag{8}$$

$$F(a_1,a_2,a_3,a_4,a_5,a_6,a_7,a_8,a_9) = \int \frac{[d^Dk_1][d^Dk_2][d^Dk_3]}{k_1^{2a_1}(k_1+k_2+k_3+p)^{2a_2}(k_1+k_2+p)^{2a_3}(k_1+k_3+p)^{2a_4}}$$
$$\times \frac{1}{k_2^{2a_5}k_3^{2a_6}(k_2^2+2k_2p)^{a_7}(k_3^2+2k_3p)^{a_8}(2k_2k_3)^{a_9}} \tag{9}$$

$$G(a_1,a_2,a_3,a_4,a_5,a_6,a_7,a_8,a_9) = \int \frac{[d^Dk_1][d^Dk_2][d^Dk_3]}{k_1^{2a_1}(k_1+k_2+p)^{2a_2}(k_1+k_2+k_3+p)^{2a_3}(k_2^2+2k_2p)^{a_4}}$$

$$\times \frac{1}{[(k_2+k_3+p)^2+1]^{a_5}(k_3^2+2k_3p)^{a_6}k_2^{2a_7}k_3^{2a_8}(2k_1p)^{a_9}} \tag{10}$$

$$H(a_1,a_2,a_3,a_4,a_5,a_6,a_7,a_8,a_9) = \int \frac{[d^Dk_1][d^Dk_2][d^Dk_3]}{k_1^{2a_1}(k_1+k_2+p)^{2a_2}(k_1+k_3+p)^{2a_3}k_2^{2a_4}k_3^{2a_5}(k_2^2+2k_2p)^{a_6}} \times \frac{1}{(k_3^2+2k_3p)^{a_7}(k_2-k_3)^{2a_8}(2k_1p)^{a_9}} \tag{11}$$

$$I(a_1,a_2,a_3,a_4,a_5,a_6,a_7,a_8,a_9) = \int \frac{[d^Dk_1][d^Dk_2][d^Dk_3]}{k_1^{2a_1}(k_1+p)^{2a_2}(k_1+k_2+p)^{2a_3}(k_2^2+2k_2p)^{a_4}(k_3^2+2k_3p)^{a_5}} \times \frac{1}{k_2^{2a_6}k_3^{2a_7}(k_2-k_3)^{2a_8}(2k_1k_3)^{a_9}} \tag{12}$$

For the decay rate calculation, we need the imaginary parts of these integrals, obtained by setting $p^2 = -1 + i0$. For the exponent a_9 we only need non-positive values; it refers to a product of momenta that may remain in the numerator after canceling scalar products against denominator factors.

In order to specify the boundary conditions of the recurrence relations, we need 24 master integrals. They vary greatly in their complexity, but for completeness, we shall list them all. Some of these integrals — particularly those with six or fewer lines — are used by more than one of the topologies and thus any descriptions we provide using the integral labels A through I are not necessarily unique. $\mathcal{F}$ denotes the loop factor $\Gamma(1+\epsilon)/(4\pi)^{D/2}$.

Five of the master integrals can be solved in closed form to all orders in ϵ via a sequence of simple one-loop integrals:

$$\mathrm{Im}\left(\int \frac{[d^Dk_1]}{k_1^2(k_1+p)^2}\int \frac{[d^Dk_2]}{(k_2^2+1)}\int \frac{[d^Dk_3]}{(k_3^2+1)}\right) = \pi\mathcal{F}^3\left[\frac{1}{\epsilon^2}+\frac{4}{\epsilon}+\left(11-\frac{\pi^2}{3}\right)+\left(26-\frac{4\pi^2}{3}-2\zeta_3\right)\epsilon + \left(57-\frac{11\pi^2}{3}-8\zeta_3+\frac{\pi^4}{90}\right)\epsilon^2+\mathcal{O}\left(\epsilon^3\right)\right], \tag{13}$$

$$\mathrm{Im}\left(\int \frac{[d^Dk_1][d^Dk_2]}{k_1^2k_2^2(k_1+k_2+p)^2}\int \frac{[d^Dk_3]}{(k_3^2+1)}\right) = \pi\mathcal{F}^3\left[-\frac{1}{2\epsilon}-\frac{15}{4}+\left(-\frac{145}{8}+\frac{\pi^2}{2}\right)\epsilon + \left(-\frac{1155}{16}+\frac{15\pi^2}{4}+5\zeta_3\right)\epsilon^2 + \left(-\frac{8281}{32}+\frac{145\pi^2}{8}+\frac{75\zeta_3}{2}-\frac{7\pi^4}{60}\right)\epsilon^3+\mathcal{O}\left(\epsilon^4\right)\right], \tag{14}$$

$$\mathrm{Im}\left(\int \frac{[d^Dk_1][d^Dk_2][d^Dk_3]}{k_1^2k_2^2k_3^2(k_1+k_2+k_3+p)^2}\right) = \pi\mathcal{F}^3\left[\frac{1}{12}+\frac{71}{72}\epsilon+\left(\frac{3115}{432}-\frac{\pi^2}{6}\right)\epsilon^2 + \left(\frac{109403}{2592}-\frac{71\pi^2}{36}-\frac{7\zeta_3}{3}\right)\epsilon^3 + \left(\frac{3386467}{15552}-\frac{3115\pi^2}{216}-\frac{497\zeta_3}{18}+\frac{4\pi^4}{45}\right)\epsilon^4+\mathcal{O}\left(\epsilon^5\right)\right], \tag{15}$$

$$\mathrm{Im}\left(\int \frac{[d^Dk_1][d^Dk_2][d^Dk_3]}{(k_1+p)^2(k_1+k_2)^2(k_1+k_3)^2k_2^2k_3^2}\right) = \pi\mathcal{F}^3\left[\frac{1}{\epsilon}+10+\left(64-2\pi^2\right)\epsilon+\left(336-20\pi^2-22\zeta_3\right)\epsilon^2 + \left(1584-128\pi^2-220\zeta_3+\frac{7\pi^4}{6}\right)\epsilon^3+\mathcal{O}\left(\epsilon^4\right)\right], \tag{16}$$

$$\mathrm{Im}\left(\int \frac{[d^Dk_1]}{k_1^2(k_1+p)^2}\int \frac{[d^Dk_2][d^Dk_3]}{k_2^2k_3^2[(k_1+k_2+p)^2+1]}\right) = \pi\mathcal{F}^3\left[-\frac{1}{2\epsilon^2}-\frac{9}{4\epsilon}+\left(-\frac{47}{8}-\frac{\pi^2}{6}\right)+\left(-\frac{133}{16}-\frac{3\pi^2}{4}-3\zeta_3\right)\epsilon + \left(\frac{417}{32}-\frac{47\pi^2}{24}-\frac{27\zeta_3}{2}-\frac{\pi^4}{4}\right)\epsilon^2+\mathcal{O}\left(\epsilon^3\right)\right]. \tag{17}$$

Two more master integrals are also a sequence of one-loop integrals, except that the final one-loop integral is less trivial:

$$\mathrm{Im}\left(\int \frac{[d^Dk_1][d^Dk_2][d^Dk_3]}{[(k_1+p)^2+1](k_1+k_2)^2(k_1+k_3+p)^2k_2^2k_3^2}\right) = \pi\mathcal{F}^3\left[\left(\frac{7}{4}-\frac{\pi^2}{6}\right)+\left(\frac{175}{8}-\frac{3\pi^2}{4}-11\zeta_3\right)\epsilon \tag{18}\right.$$

$$\left. + \left(\frac{2681}{16}-\frac{131\pi^2}{24}-\frac{99\zeta_3}{2}-\frac{29\pi^4}{60}\right)\epsilon^2+\mathcal{O}\left(\epsilon^3\right)\right],$$

$$\text{Im}\left(\int \frac{[d^Dk_1][d^Dk_2][d^Dk_3]}{k_1^2[(k_1+p)^2+1](k_1+k_2+k_3+p)^2k_2^2k_3^2}\right) = \pi\mathcal{F}^3\left[\frac{1}{4}+\frac{25}{8}\epsilon+\left(\frac{383}{16}-\frac{\pi^2}{2}\right)\epsilon^2+\mathcal{O}\left(\epsilon^3\right)\right] . \tag{19}$$

One of the master integrals requires the real part of the two-loop massive self-energy integral first evaluated in [20]:

$$\begin{aligned}\text{Im}\left(\int \frac{[d^Dk_1]}{k_1^2(k_1+p)^2}\int \frac{[d^Dk_2][d^Dk_3]}{(k_2^2+1)(k_3^2+1)[(k_2+k_3+p)^2+1]}\right) = \pi\mathcal{F}^3\Bigg[&-\frac{3}{2\epsilon^2}-\frac{29}{4\epsilon}+\left(-\frac{175}{8}+\frac{\pi^2}{2}\right)\\ &+\left(-\frac{765}{16}+\frac{13\pi^2}{12}+3\zeta_3\right)\epsilon\\ &+\left(-\frac{1943}{32}-\frac{97\pi^2}{24}-\frac{27\zeta_3}{2}-\frac{\pi^4}{60}+8\pi^2\ln 2\right)\epsilon^2+\mathcal{O}\left(\epsilon^3\right)\Bigg] .\end{aligned} \tag{20}$$

Five of the master integrals are only needed to leading order in our calculations and are very closely related to some of the four-loop integrals calculated for muon decay in [19]. Specifically, if the massless neutrino-electron loop is integrated out, an overall factor of $B(1-\epsilon,1-\epsilon)\mathcal{F}/\epsilon$ is obtained and the exponent on the W line increases from 1 to $(1+\epsilon)$. To leading order in ϵ, neither this modification to the W exponent nor the difference in the normalization conventions changes the master integral, and so after converting the appropriate results from Minkowski space to Euclidean space, we conveniently obtain the following master integrals:

$$\text{Im}\ A(1,1,0,1,1,1,1,1,0) = \pi\mathcal{F}^3\left[\frac{\pi^4}{18}+\mathcal{O}\left(\epsilon\right)\right] , \tag{21}$$

$$\text{Im}\ B(1,1,1,1,1,1,1,1,-1) = \pi\mathcal{F}^3\left[\frac{17\pi^4}{720}+\mathcal{O}\left(\epsilon\right)\right] , \tag{22}$$

$$\text{Im}\ E(1,0,1,1,1,1,1,1,0) = \pi\mathcal{F}^3\left[\frac{\pi^4}{15}+\mathcal{O}\left(\epsilon\right)\right] , \tag{23}$$

$$\text{Im}\ F(1,1,1,1,0,0,1,1,0) = \pi\mathcal{F}^3\left[\left(-2+\frac{\pi^2}{6}+\frac{13\zeta_3}{4}-\frac{\pi^2}{2}\ln 2\right)+\mathcal{O}\left(\epsilon\right)\right] , \tag{24}$$

$$\text{Im}\ F(1,1,1,1,1,1,1,1,-1) = \pi\mathcal{F}^3\left[-\frac{\pi^4}{60}+\mathcal{O}\left(\epsilon\right)\right] . \tag{25}$$

The other integrals in [19] are also relevant to our calculation, however, since we require analytic results beyond the leading order in ϵ for the remaining master integrals, we can only use these four-loop integrals as a consistency check on our own calculations. The remaining eleven master integrals are:

$$\begin{aligned}\text{Im}\left(\int \frac{[d^Dk_1][d^Dk_2][d^Dk_3]}{[k_1^2+1](k_1+k_2)^2k_2^2k_3^2(k_2+k_3+p)^2}\right) = \pi\mathcal{F}^3\Bigg[&\frac{1}{2\epsilon}+\frac{15}{4}+\left(\frac{145}{8}-\frac{\pi^2}{2}\right)\epsilon\\ &+\left(\frac{1155}{16}-\frac{15\pi^2}{4}-5\zeta_3\right)\epsilon^2+\mathcal{O}\left(\epsilon^3\right)\Bigg] ,\end{aligned} \tag{26}$$

$$\begin{aligned}\text{Im}\left(\int \frac{[d^Dk_1][d^Dk_2][d^Dk_3]}{k_1^2(k_1+p)^2k_2^2k_3^2[(k_1+k_2+k_3+p)^2+1]}\right) = \pi\mathcal{F}^3\Bigg[&-\frac{1}{2\epsilon^2}-\frac{5}{2\epsilon}-\frac{17}{2}+\left(-\frac{49}{2}+2\zeta_3\right)\epsilon\\ &+\left(-\frac{129}{2}+10\zeta_3\right)\epsilon^2+\mathcal{O}\left(\epsilon^3\right)\Bigg] ,\end{aligned} \tag{27}$$

$$\begin{aligned}\text{Im}\left(\int \frac{[d^Dk_1][d^Dk_2][d^Dk_3]}{(k_1+p)^2(k_1+k_2)^2(k_1+k_3)^2k_2^2(k_3^2+1)}\right) = \pi\mathcal{F}^3\Bigg[&\frac{1}{2\epsilon}+\left(\frac{11}{2}-\frac{\pi^2}{6}\right)+\left(\frac{77}{2}-\frac{3\pi^2}{2}-8\zeta_3\right)\epsilon\\ &+\left(\frac{439}{2}-\frac{19\pi^2}{2}-53\zeta_3-\frac{3\pi^4}{10}\right)\epsilon^2+\mathcal{O}\left(\epsilon^3\right)\Bigg] .\end{aligned} \tag{28}$$

$$\text{Im}\ B(1,1,1,0,1,1,0,1,0) = \pi\mathcal{F}^3\left[\frac{1}{2\epsilon^2}+\frac{7}{2\epsilon}+\left(\frac{33}{2}-\frac{\pi^2}{3}-2\zeta_3\right)+\left(\frac{131}{2}-\frac{7\pi^2}{3}-10\zeta_3-\frac{7\pi^4}{180}\right)\epsilon+\mathcal{O}\left(\epsilon^2\right)\right] , \tag{29}$$

$$\begin{aligned}\text{Im}\ B(1,1,1,1,1,2,0,0,0) = \pi\mathcal{F}^3\Bigg[&\left(-\frac{5\zeta_3}{4}+\frac{\pi^2}{2}\ln 2\right)\\ &+\left(-\frac{5\zeta_3}{2}+\frac{11\pi^4}{240}+\pi^2\ln 2+\frac{\pi^2}{3}\ln^2 2-\frac{1}{3}\ln^4 2-8\text{Li}_4(1/2)\right)\epsilon+\mathcal{O}\left(\epsilon^2\right)\Bigg] ,\end{aligned} \tag{30}$$

$$\text{Im } B(1,1,1,1,2,2,0,0,0) = \pi\mathcal{F}^3\left[\frac{\pi^2}{12}+\left(\frac{\pi^2}{6}-\frac{3\zeta_3}{4}+\frac{\pi^2}{2}\ln 2\right)\epsilon\right.$$
$$\left.+\left(\frac{\pi^2}{3}-\frac{3\zeta_3}{2}+\frac{11\pi^4}{180}+\pi^2\ln 2+\frac{\pi^2}{3}\ln^2 2-\frac{1}{3}\ln^4 2-8\text{Li}_4(1/2)\right)\epsilon^2+\mathcal{O}\left(\epsilon^3\right)\right] , \quad (31)$$

$$\text{Im } C(1,0,1,1,0,1,1,1,0) = \pi\mathcal{F}^3\left[1+(14-4\zeta_3)\,\epsilon+\left(119-\pi^2-28\zeta_3-\frac{\pi^4}{3}\right)\epsilon^2+\mathcal{O}\left(\epsilon^3\right)\right] , \quad (32)$$

$$\text{Im } C(1,1,1,0,1,1,1,0,0) = \pi\mathcal{F}^3\left[\frac{1}{2\epsilon^2}+\frac{5}{2\epsilon}+\left(\frac{15}{2}-\frac{\pi^2}{6}-2\zeta_3\right)+\left(\frac{29}{2}-\frac{\pi^2}{6}-9\zeta_3+\frac{\pi^4}{60}\right)\epsilon+\mathcal{O}\left(\epsilon^2\right)\right] , \quad (33)$$

$$\text{Im } F(1,1,0,0,1,1,1,1,0) = \pi\mathcal{F}^3\left[\left(-1+\frac{\pi^2}{6}\right)+\left(-14+\frac{7\pi^2}{6}+9\zeta_3\right)\epsilon\right.$$
$$\left.+\left(-119+\frac{15\pi^2}{2}+63\zeta_3+\frac{41\pi^4}{180}\right)\epsilon^2+\mathcal{O}\left(\epsilon^3\right)\right] , \quad (34)$$

$$\text{Im } F(1,1,0,1,0,1,1,1,0) = \pi\mathcal{F}^3\left[\frac{1}{\epsilon}+\left(11-\frac{\pi^2}{6}-\zeta_3\right)+\left(77-\frac{13\pi^2}{6}-13\zeta_3-\frac{7\pi^4}{90}\right)\epsilon+\mathcal{O}\left(\epsilon^2\right)\right] , \quad (35)$$

$$\text{Im } G(1,1,1,0,1,1,1,0,0) = \pi\mathcal{F}^3\left[\left(1-\frac{\pi^2}{6}+\zeta_3\right)+\left(14-\frac{7\pi^2}{6}-3\zeta_3+\frac{\pi^4}{18}\right)\epsilon+\mathcal{O}\left(\epsilon^2\right)\right] . \quad (36)$$

The integrals in Eqs. (30) and (31) contain the fourth-order Polylogarithm $\text{Li}_4(1/2) = 0.517479\ldots$, along with terms with higher powers of $\ln 2$. None of these constants appear in our final results, which suggests that there might exist a basis of master integrals in which these constants do not arise in any of the terms at the orders in ϵ which contribute to our final results.

IV. EVALUATION OF MASTER INTEGRALS

The eleven master integrals in Eqs. (26) through (36) were evaluated on a case-by-case basis by integrating the phase space of massless propagators severed by cuts. In this section, we will illustrate the procedure with a few examples. We will compute master integrals having two-, three-, and four-particle cuts, respectively.

The general procedure is as follows. For any particular integral, we can use the optical theorem to obtain its imaginary part via

$$\text{Im}\,\mathcal{M} = \frac{1}{2}\sum_{\text{cuts}}\int d\Pi_{\text{cut}}\ \mathcal{M}_1\mathcal{M}_2^* , \quad (37)$$

where $\mathcal{M}_1$ and $\mathcal{M}_2$ are the scalar amplitudes arising from the uncut propagators on the two sides of the cut, the cut propagators are assumed to be on mass shell, and $\int d\Pi_{\text{cut}}$ is the integral over the phase space of the cut propagators. Working in dimensional regularization, the phase space integral involves a factor of

$$\frac{d^{D-1}\mathbf{q}}{(2\pi)^{D-1}2E} \quad (38)$$

for every particle involved in a given cut, along with a D-dimensional δ-function to conserve overall four-momentum. Much of the phase space integration can be done for a general case without assuming anything about the amplitudes $\mathcal{M}_1$ and $\mathcal{M}_2$, so that the phase space integrals relevant to an n-particle cut can be reduced to simpler integrals involving a small number of scalar parameters. We shall see this explicitly in the following three examples, each with a different number of cut particle lines.

A. Example 1: two-particle cut

Our first example will be the integral of Eq. (30). As can be seen in the sketch of Fig. 3, there is a single cut (through the two rightmost propagators) that can be made through massless lines in the diagram. The two-body phase space integral for massless particles is especially simple, since the two particles must emerge back-to-back while partitioning the total energy equally. Defining the general phase-space factor by

$$\mathbf{P_n} = \int\prod_{i=1}^{n}\frac{\mathrm{d}^{D-1}\mathbf{p}_i}{(2\pi)^{D-1}2E_i}\,(2\pi)^D\delta^D\left(p-\sum_{j=1}^{n}p_j\right) , \quad (39)$$

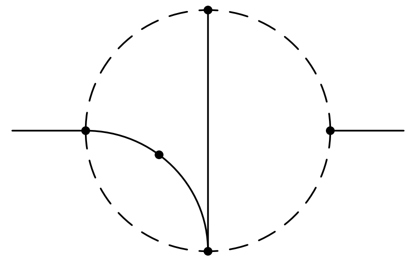

FIG. 3: Sketch of the master integral $B(1,1,1,1,1,2,0,0,0)$. The imaginary part of this integral can be obtained from a two-particle cut through the massless lines on the right side of the diagram. Solid and dashed lines depict massive and massless propagators, respectively.

an explicit calculation leads to the two-body phase space factor

$$\mathbf{P_2} = \frac{\mathcal{F}\ \ 2^{2\epsilon}\pi^{3/2}}{\Gamma(1+\epsilon)\Gamma(3/2-\epsilon)} \ , \tag{40}$$

where, as before, $\mathcal{F}$ denotes the loop factor $\Gamma(1+\epsilon)/(4\pi)^{D/2}$. There are no remaining integrals in this expression, and so we have

$$\text{Im } B(1,1,1,1,1,2,0,0,0) = \frac{\mathbf{P_2}}{2}\ L_1 \ , \tag{41}$$

where L_1 is the factor arising from the two-loop integral for the three-point function to the left of the cut in Fig. 3. Explicitly,

$$L_1 = \int \frac{[d^D k][d^D l]}{(k+p)^2[(k+p-q)^2+1][(k+l)^2+1]^2 l^2} \ , \tag{42}$$

where k and l are the loop momenta, p is the incoming momentum from the left (with the onshell condition $p^2=-1$), q emerges onto the massless line on the upper-right ($q^2=0$), and $(p-q)$ emerges onto the massless line on the lower-right (such that $(p-q)^2=0$). Applying the Feynman parameters x, y, and z in three consecutive stages, we can evaluate the l- and k-integrals so that we are left with the parametric integral

$$L_1 = \mathcal{F}^2\ \frac{\Gamma(1+2\epsilon)}{\Gamma^2(1+\epsilon)} \int_0^1 dx \int_0^1 dy \int_0^1 dz\ \frac{x^\epsilon(1-x)^{-\epsilon} z(1-z)^\epsilon}{\left[z^2xy+zx(1-2y)+1-z\right]^{1+2\epsilon}} \ . \tag{43}$$

The y-integral can be solved explicitly, but the remaining x- and z-integrals are more difficult. The integral is finite (as a result of our use of a second factor of one of the massive lines) and thus we can expand the integrand in ϵ using expressions like

$$x^\epsilon = 1 + \epsilon \ln x + \frac{\epsilon^2}{2}\ln^2 x + \mathcal{O}\left(\epsilon^3\right) \ , \tag{44}$$

and then evaluate the integrals order by order in ϵ. The leading (ϵ^0) term is relatively simple, but the presence of products of logarithms in the subsequent terms quickly escalates the level of difficulty. The FORM packages Summer [21] and Harmpol [22] have proven to be very useful for evaluating some of these integrals; some of the related formulas are conveniently tabulated in [23]. For the first two terms of L_1, we obtain

$$L_1 = \mathcal{F}^2\left[\left(-\frac{5\zeta_3}{4}+\frac{\pi^2}{2}\ln 2\right)+\left(-\frac{5\zeta_3}{2}+\frac{11\pi^4}{240}+\pi^2\ln 2+\frac{\pi^2}{3}\ln^2 2-\frac{1}{3}\ln^4 2-8\text{Li}_4(1/2)\right)\epsilon+\mathcal{O}\left(\epsilon^2\right)\right] \ , \tag{45}$$

and, in conjunction with Eqs. (40) and (41), thereby establish the result in Eq. (30).

B. Example 2: three-particle cut

An example of a master integral requiring a three-particle cut is Eq. (35). This integral is sketched in Fig. 4, where it is seen that a diagonal cut through the massless lines leaves a one-loop amplitude to the left of the cut and a

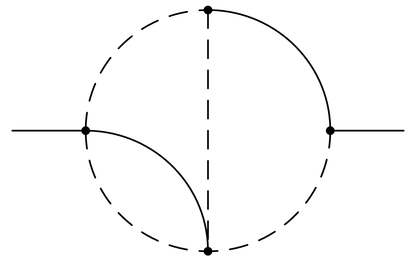

FIG. 4: Sketch of the master integral $F(1,1,0,1,0,1,1,1,0)$. The imaginary part of this integral can be obtained from a three-particle cut through the massless lines from the upper left side of the diagram towards the lower right.

single massive propagator to the right. The three massless particles that we cut through can be put on shell with a range of relative kinematic configurations, meaning that the three-body phase space integral can only be partially solved in advance. The remainder of the integral will be over two kinematic parameters (such as the energies of two of the particles) upon which the amplitudes $\mathcal{M}_1$ and $\mathcal{M}_2$ might also depend. A very convenient formulation of the three-body phase space involves the use of the relativistic invariants

$$u = (q_1 + q_3)^2 \qquad \text{and} \qquad z = (q_2 + q_3)^2 \tag{46}$$

as the integration variables. This leads to the expression

$$\mathbf{P_3} = \frac{(\mathbf{P_2})^2}{2\pi B_{11}} \int_0^1 dz \int_0^{1-z} du \; u^{-\epsilon} \; z^{-\epsilon} \; (1-z-u)^{-\epsilon} \; , \tag{47}$$

where $B_{11} = B(1-\epsilon, 1-\epsilon)$. Returning to the master integral in Fig. 4, we observe that the massive propagator ($m = 1$) in the upper right part of the diagram splits directly into two onshell massless particles, and thus the momentum q flowing through this propagator is related to one of our invariants:

$$(q^2+1)^{-1} \longrightarrow (1-z)^{-1} \; . \tag{48}$$

In addition, we must include a factor in the phase space integral resulting from the one-loop integral in the lower left portion of Fig. 4. The momentum l flowing through this diagram is related to the other invariant via $l^2 = -u$, and the loop integral can quickly be evaluated with a Feynman parameter:

$$\int \frac{[d^D k]}{[(k+l)^2+1]k^2} = \frac{\mathcal{F}}{\epsilon} \int_0^1 dx \; (1-x)^{-\epsilon} (1-xu)^{-\epsilon} \; . \tag{49}$$

Substituting this expression into Eq. (47), we have

$$\text{Im } F(1,1,0,1,0,1,1,1,0) = \frac{\mathcal{F} \; (\mathbf{P_2})^2}{4\pi\epsilon B_{11}} J \; , \tag{50}$$

where J denotes the 3-parameter integral:

$$J = \int_0^1 dx \int_0^1 dz \int_0^{1-z} du \; \frac{(1-x)^{-\epsilon} \; u^{-\epsilon} \; z^{-\epsilon} \; (1-z-u)^{-\epsilon} \; (1-xu)^{-\epsilon}}{(1-z)} \; . \tag{51}$$

As in the previous example, this integral is finite, and hence we can safely expand the integrand in ϵ and evaluate it term by term. The result,

$$J = 1 + \left(9 - \frac{\pi^2}{6} - \zeta_3\right)\epsilon + \left(55 - \frac{4\pi^2}{3} - 11\zeta_3 - \frac{7\pi^4}{90}\right)\epsilon^2 + \mathcal{O}\left(\epsilon^3\right) \; , \tag{52}$$

once folded in with the other factors in Eq. (50), leads to the expression of Eq. (35).

C. Example 3: four-particle cut

Our final example illustrates how a four-particle cut can be used to obtain Eq. (34). This integral is sketched in Fig. 5. On each side of the cut we have a massive propagator. As might be expected when cutting through four lines

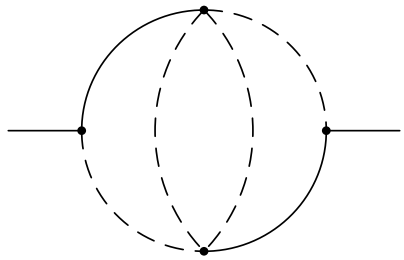

FIG. 5: Sketch of the master integral $F(1,1,0,0,1,1,1,1,0)$. The imaginary part of this integral can be obtained from a four-particle cut through the massless lines.

in a planar three-loop diagram, there are no loop integrals remaining. The most general expression for a four-body phase space integral is extremely complicated, but it happens that we can obtain a simpler expression suitable for our purposes by modifying the three-body result. Specifically, the generalization of the three-body phase space integral in Eq. (47) from the case of three massless particles to the case of two massless particles and a particle of squared-mass $y = q_2^2$ (such that $0 \leq y \leq 1$) leads to

$$\mathbf{P_{3m}} = \frac{(\mathbf{P_2})^2}{2\pi B_{11}} \int_0^1 dz \int_0^{1-z} du\ u^{-\epsilon}\ z^{-\epsilon}\ \left(\frac{(1-z)(z-y)}{z} - u\right)^{-\epsilon} . \tag{53}$$

When $y = 0$, this reduces to Eq. (47), but if we interpret y as the relativistic invariant of a pair of massless particles in a four-body phase space,

$$y = (q_2 + q_4)^2 , \tag{54}$$

we obtain a four-body phase space integral

$$\mathbf{P_4} = \frac{(\mathbf{P_2})^3}{4\pi^2 B_{11}} \int_0^1 dz \int_0^{1-z} du \int_0^{z(1-z-u)/(1-z)} dy\ u^{-\epsilon}\ z^{-\epsilon}\ y^{-\epsilon}\ \left(\frac{(1-z)(z-y)}{z} - u\right)^{-\epsilon} \tag{55}$$

that is applicable to certain integrals where two of the massless particles form a subloop. In order to evaluate the integral in Fig. 5, we will need to replace the invariant $u = (q_1+q_3)^2$ with $v = (q_1+q_2)^2$ since the massless loop corresponds to a massive q_2 and thus the massive propagators beside the cut carry momenta (q_1+q_2) and (q_2+q_3). With

$$u + v + z = 1 + y , \tag{56}$$

Eq. (55) can be rewritten as

$$\mathbf{P_4} = \frac{(\mathbf{P_2})^3}{4\pi^2 B_{11}} \int_0^1 dy \int_y^1 dz \int_{y/z}^{1+y-z} dv\ y^{-\epsilon}\ z^{-\epsilon}\ (1+y-z-v)^{-\epsilon}\ \left(v - \frac{y}{z}\right)^{-\epsilon} . \tag{57}$$

The integral we need to evaluate has the additional propagator factors $(1-v)^{-1}$ and $(1-z)^{-1}$, and as before, can be expanded in ϵ and evaluated term by term, thereby leading to the result of Eq. (34).

V. RESULTS

The QCD corrections to the decay width for $t \to bW$ can be written as

$$\Gamma(t \to bW) = \Gamma_0 \left[X_0 + \frac{\alpha_s}{\pi} X_1 + \left(\frac{\alpha_s}{\pi}\right)^2 X_2 + \mathcal{O}\left(\alpha_s^3\right)\right] , \tag{58}$$

where

$$\Gamma_0 = \frac{G_F \left|V_{tb}\right|^2 m_t^3}{8\sqrt{2}\pi} , \tag{59}$$

is the tree-level decay width in the limit that $m_W = 0$. The results for X_0 and X_1 are known analytically [24, 25].

The two-loop contribution with which we are presently concerned, X_2, has been estimated numerically [26, 27]. Detailed comparisons of our analytical results with those studies is given in [1]. We divide X_2 into four gauge-invariant color structures,

$$X_2 = C_F\left(T_R N_L X_L + T_R N_H X_H + C_F X_A + C_A X_{NA}\right) \ . \tag{60}$$

Here we use $SU(N)$ factors (with $N=3$) $C_F = (N^2-1)/(2N)$, $C_A = N$, and $T_R = 1/2$. N_L denotes the number of massless quark species and N_H that of quarks with the mass equal to that of the decaying quark. Defining the parameter $\omega = m_W^2/m_t^2$, our results for the four classes of contributions in Eq. (60) are:

$$\begin{aligned} X_L = & \left[-\frac{4}{9}+\frac{23\pi^2}{108}+\zeta_3\right]+\omega\left[-\frac{19}{6}+\frac{2\pi^2}{9}\right]+\omega^2\left[\frac{745}{72}-\frac{31\pi^2}{36}-3\zeta_3-\frac{7}{4}\ln\omega\right] \\ & +\omega^3\left[-\frac{5839}{648}+\frac{7\pi^2}{27}+2\zeta_3+\frac{5}{3}\ln\omega\right]+\omega^4\left[\frac{4253}{8640}+\frac{\pi^2}{4}-\frac{17}{144}\ln\omega\right] \\ & +\omega^5\left[-\frac{689}{27000}+\frac{\pi^2}{15}-\frac{7}{900}\ln\omega\right]+\omega^6\left[-\frac{13187}{181440}+\frac{\pi^2}{36}+\frac{1}{48}\ln\omega\right] \\ & +\omega^7\left[-\frac{2282381}{37044000}+\frac{\pi^2}{70}+\frac{2263}{88200}\ln\omega\right]+\mathcal{O}\left(\omega^8\right) \ , \end{aligned} \tag{61}$$

$$\begin{aligned} X_H = & \left[\frac{12991}{1296}-\frac{53\pi^2}{54}-\frac{\zeta_3}{3}\right]+\omega\left[-\frac{35}{108}-\frac{4\pi^2}{9}+4\zeta_3\right]+\omega^2\left[-\frac{6377}{432}+\frac{25\pi^2}{18}+\zeta_3\right] \\ & +\omega^3\left[\frac{319}{27}-\frac{31\pi^2}{27}-\frac{2\zeta_3}{3}\right]+\omega^4\left[\frac{76873}{8640}-\frac{8\pi^2}{9}\right]+\omega^5\left[\frac{237107}{27000}-\frac{8\pi^2}{9}\right]+\mathcal{O}\left(\omega^6\right) \ , \end{aligned} \tag{62}$$

$$\begin{aligned} X_A = & \left[5-\frac{119\pi^2}{48}-\frac{53\zeta_3}{8}-\frac{11\pi^4}{720}+\frac{19}{4}\pi^2\ln 2\right]+\omega\left[-\frac{73}{8}+\frac{41\pi^2}{8}-\frac{41\pi^4}{90}\right] \\ & +\omega^2\left[-\frac{7537}{288}+\frac{523\pi^2}{96}+\frac{295\zeta_3}{32}-\frac{191\pi^4}{720}-\frac{27}{16}\pi^2\ln 2+\left(\frac{115}{48}-\frac{5\pi^2}{16}\right)\ln\omega\right] \\ & +\omega^3\left[\frac{16499}{864}-\frac{407\pi^2}{216}-\frac{7\zeta_3}{2}+\frac{7\pi^4}{120}-\pi^2\ln 2+\left(-\frac{367}{144}+\frac{5\pi^2}{9}\right)\ln\omega\right] \\ & +\omega^4\left[-\frac{1586479}{259200}+\frac{2951\pi^2}{6912}+\frac{9\zeta_3}{2}+\left(\frac{31979}{17280}-\frac{\pi^2}{16}\right)\ln\omega\right] \\ & +\omega^5\left[-\frac{11808733}{6480000}+\frac{37\pi^2}{2400}+\frac{6\zeta_3}{5}+\left(\frac{13589}{27000}-\frac{\pi^2}{60}\right)\ln\omega\right]+\mathcal{O}\left(\omega^6\right) \ , \end{aligned} \tag{63}$$

$$\begin{aligned} X_{NA} = & \left[\frac{521}{576}+\frac{505\pi^2}{864}+\frac{9\zeta_3}{16}+\frac{11\pi^4}{1440}-\frac{19}{8}\pi^2\ln 2\right]+\omega\left[\frac{91}{48}+\frac{329\pi^2}{144}-\frac{13\pi^4}{60}\right] \\ & +\omega^2\left[-\frac{12169}{576}+\frac{2171\pi^2}{576}+\frac{377\zeta_3}{64}-\frac{77\pi^4}{288}+\frac{27}{32}\pi^2\ln 2+\left(\frac{73}{16}-\frac{3\pi^2}{32}\right)\ln\omega\right] \\ & +\omega^3\left[\frac{13685}{864}-\frac{47\pi^2}{72}-\frac{19\zeta_3}{4}+\frac{43\pi^4}{720}+\frac{1}{2}\pi^2\ln 2+\left(-\frac{1121}{432}-\frac{\pi^2}{6}\right)\ln\omega\right] \\ & +\omega^4\left[-\frac{420749}{103680}-\frac{3263\pi^2}{13824}-\frac{9\zeta_3}{8}+\left(\frac{11941}{6912}-\frac{3\pi^2}{32}\right)\ln\omega\right] \\ & +\omega^5\left[-\frac{4868261}{12960000}-\frac{557\pi^2}{4800}-\frac{3\zeta_3}{10}+\left(\frac{153397}{216000}-\frac{\pi^2}{40}\right)\ln\omega\right]+\mathcal{O}\left(\omega^6\right) \ . \end{aligned} \tag{64}$$

As discussed in [1], we obtain the two-loop QCD correction to the top quark decay width by substituting $\omega \simeq 0.213$ into these expressions. There are already sufficiently many terms so as to render the theoretical uncertainty 20 times smaller than the experimental uncertainty induced by the mass measurements of the top quark. Furthermore, these expressions can be smoothly matched to the corresponding expressions [4] for the two-loop QCD corrections to the semileptonic decay $b \to u\ell\nu$ in the zero recoil limit. The result of such a matching procedure is depicted in Fig. 6.

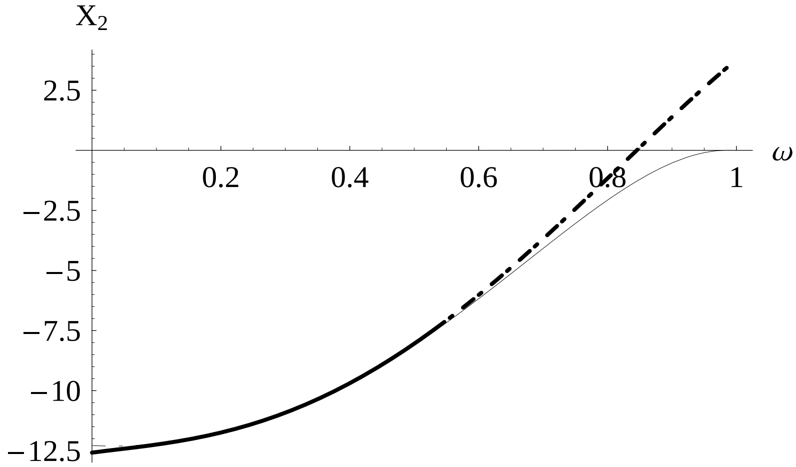

FIG. 6: Matching of expansions around $\omega = 0$ (thick line) and $\omega = 1$ (thin line). The solid line denotes the resulting correction to the decay width valid in the full range of ω.

VI. CONCLUSIONS

We have presented an analytical approach to next-to-next-to-leading order studies of heavy-to-light decays. We have used top quark decay as an illustrative example here; in [1] we also studied the distribution of the lepton invariant mass in the semileptonic $b \to u$ decay and have reproduced the $\mathcal{O}\left(\alpha^2\right)$ corrections to the muon lifetime. A number of other phenomenologically interesting studies become possible with the results presented here. For example, corrections to radiative $b \to s\gamma$ decays and to $B_{d,s}$ meson mixing require matrix elements of very similar if not identical kinematic structure. (For the mixing, one can expand in the four-momentum carried by the light quark and obtain propagator-like diagrams studied in the present paper.)

We employed two approaches to reducing Feynman integrals to a basis set of primitive ones. In both we use integration-by-parts recurrence relations that we either solve completely, or for a targeted set of needed integrals.

The most appealing feature of the targeted approach is that the core of the program is universal for all topologies. Unlike the complete solution method, where each new topology necessitates a by-hand construction of a new solution algorithm, the targeted approach needs only a minimal specification of the topology under consideration. As a result, once the program core is written and tested, very little programming is needed to incorporate new topologies, thereby saving time, effort, and minimizing the likelihood of programming bugs.

Another major difference between the two approaches is the use of subtopologies. In the traditional method, the removal of a line will often facilitate a mapping of a loop integral from a more complex topology onto a simpler topology, for which a new set of identities is used. The drawback to this intuitively reasonable process is a proliferation in the number of topologies to be programmed. For example, the 9 master topologies that we encounter in this work (discussed in section III) require approximately 40 additional subtopologies. The targeted approach, on the other hand, only needs to deal with the master topologies, as it is able to solve a given topology completely using only one set of identities. At the three-loop level, it would be very difficult for a human to program an algorithm in this way.

A key feature of the targeted approach is the generation of large tables containing all possible integrals in a topology with a predetermined range of powers. Once this table is generated, it is accessed by the programs responsible for assembling a particular physical calculation. In the complete method, conversely, the algorithms are typically applied in real-time, and the generation of dynamic tables will likely be used in the near future to improve the performance of this approach. Given the large range of powers which can arise when performing a calculation using asymptotic expansions, these tables and intermediate expressions can become quite large.

In summary, the targeted approach appears to be superior by virtue of saving human time. The burden is shifted to the computer and thus an efficient implementation of the algorithm is essential. We developed the project-specific software based on the BEAR package [28]. The targeted approach has also recently been implemented in MAPLE [29].

The availability of the targeted approach greatly simplifies multiloop calculations. The remaining bottleneck involves the evaluation of master integrals. Further progress in perturbative calculations may depend on a radically new approach addressing this issue.

APPENDIX

As described in Section V, expansion around $\omega = 0$ is given by the functions (61)–(64). The complementary expansion around $\omega = 1$ has been studied in [4]. Below, the corresponding formulae are given for completeness:

$$\begin{aligned}
X_L(\delta\simeq 0) &= \delta^2\left[-\frac{117}{8}+\frac{41}{18}\pi^2+6\zeta_3+\left(\frac{39}{4}-\frac{4}{3}\pi^2\right)\ln\delta-\frac{3}{2}\ln^2\delta\right]\\
&+\delta^3\left[\frac{797}{108}-\frac{53}{27}\pi^2-4\zeta_3+\left(-\frac{31}{18}+\frac{8}{9}\pi^2\right)\ln\delta-\frac{1}{3}\ln^2\delta\right]\\
&+\delta^4\left[\frac{1289}{432}+\frac{1}{18}\pi^2-\frac{37}{18}\ln\delta+\frac{1}{6}\ln^2\delta\right]+\delta^5\left[\frac{1817}{3600}-\frac{3}{5}\ln\delta\right]+\mathcal{O}\left(\delta^6\right)\ , \qquad (A.1)\\
X_H(\delta\simeq 0) &= \delta^2\left[\frac{133}{16}-\frac{5}{6}\pi^2\right]+\delta^3\left[-\frac{797}{216}+\frac{1}{3}\pi^2\right]+\delta^4\left[\frac{2473}{5400}-\frac{1}{36}\pi^2-\frac{1}{10}\ln\delta\right]\\
&+\delta^5\left[\frac{1747}{5400}-\frac{1}{30}\pi^2-\frac{1}{15}\ln\delta\right]+\mathcal{O}\left(\delta^6\right)\ , \qquad (A.2)\\
X_A(\delta\simeq 0) &= \delta^2\left[\frac{523}{32}-\frac{71}{12}\pi^2+\frac{7}{2}\pi^2\ln 2+\frac{8}{15}\pi^4-\frac{39}{4}\zeta_3-\left(\frac{147}{16}-2\pi^2\right)\ln\delta+\frac{27}{8}\ln^2\delta\right]\\
&+\delta^3\left[\frac{1363}{144}-\frac{217}{216}\pi^2-\frac{1}{3}\pi^2\ln 2-\frac{32}{90}\pi^4+\left(-\frac{287}{24}+\frac{5}{9}\pi^2\right)\ln\delta+\frac{15}{4}\ln^2\delta\right]\\
&+\delta^4\left[\frac{1537}{288}+\frac{937}{864}\pi^2-\frac{5}{12}\pi^2\ln 2-\left(\frac{67}{12}+\frac{17}{36}\pi^2\right)\ln\delta+\frac{17}{8}\ln^2\delta\right]\\
&+\delta^5\left[\frac{43609}{43200}+\frac{7609}{21600}\pi^2-\frac{1}{4}\zeta_3-\frac{1}{10}\pi^2\ln 2-\left(\frac{269}{90}+\frac{8}{90}\pi^2\right)\ln\delta+\frac{11}{6}\ln^2\delta\right]+\mathcal{O}\left(\delta^6\right)\ , \qquad (A.3)\\
X_{NA}(\delta\simeq 0) &= \delta^2\left[\frac{1103}{32}-\frac{881}{144}\pi^2-\frac{7}{4}\pi^2\ln 2+\frac{13}{60}\pi^4-\frac{129}{8}\zeta_3+\left(-\frac{423}{16}+\frac{47}{12}\pi^2\right)\ln\delta+\frac{33}{8}\ln^2\delta\right]\\
&+\delta^3\left[-\frac{623}{54}+\frac{247}{48}\pi^2+\frac{1}{6}\pi^2\ln 2-\frac{13}{90}\pi^4+12\zeta_3+\left(\frac{155}{72}-2\pi^2\right)\ln\delta+\frac{2}{3}\ln^2\delta\right]\\
&+\delta^4\left[-\frac{18319}{1728}-\frac{19}{572}\pi^2+\frac{5}{24}\pi^2\ln 2-\frac{1}{8}\zeta_3+\left(\frac{1877}{288}-\frac{1}{24}\pi^2\right)\ln\delta-\frac{17}{24}\ln^2\delta\right]\\
&+\delta^5\left[-\frac{52379}{43200}-\frac{5041}{43200}\pi^2+\frac{1}{20}\pi^2\ln 2-\frac{1}{40}\zeta_3+\left(\frac{139}{90}+\frac{1}{90}\pi^2\right)\ln\delta-\frac{11}{48}\ln^2\delta\right]+\mathcal{O}\left(\delta^6\right)\ , \qquad (A.4)
\end{aligned}$$

where $\delta = 1 - \omega$. These two sets of expressions can be smoothly matched in the intermediate region to produce functions valid in the full range of ω. For practical purposes it is convenient to replace this complicated combination of exact expansions by a collection of polynomial fits with numerical coefficients. We found that the following simple functions

$$\begin{aligned}
X_L &\simeq 2.854 - 0.665\,\omega - 0.109\,\omega^2 - 8.572\,\omega^3 + 5.561\,\omega^4 + 0.931\,\omega^5\ , \qquad (A.5)\\
X_H &\simeq -0.063615 + 0.098146\,\omega + 0.144642\,\omega^2 - 0.307331\,\omega^3 + 0.107417\,\omega^4 + 0.020707\,\omega^5\ , \qquad (A.6)\\
X_A &\simeq 3.575 - 2.867\,\omega + 2.241\,\omega^2 - 12.027\,\omega^3 + 11.564\,\omega^4 - 2.489\,\omega^5\ , \qquad (A.7)\\
X_{NA} &\simeq -8.151 + 2.990\,\omega - 3.537\,\omega^2 + 36.561\,\omega^3 - 42.275\,\omega^4 + 23.899\,\omega^5 - 9.494\,\omega^6\ , \qquad (A.8)
\end{aligned}$$

give a very good approximation. For any value of ω they deviate from the exact value by less than 0.01. The second order contribution to the decay rate for $N_L = 5$ and $N_H = 1$ can be written in the approximate form

$$X_2 \simeq -16.729 + 3.064\,\omega + 4.481\,\omega^2 + 35.191\,\omega^3 - 10.336\,\omega^4 - 15.655\,\omega^5, \qquad (A.9)$$

where the error introduced by the fit is smaller than the uncertainty of the result due to, for example, higher-order QCD corrections.

Acknowledgements: We thank Kirill Melnikov and Sven Moch for helpful discussions and Johannes Blümlein for sharing Ref. [23] with us.

This research was supported by the Science and Engineering Research Canada, Alberta Ingenuity, and by the Collaborative Linkage Grant PST.CLG.977761 from the NATO Science Programme.

FT thanks Andrzej Czarnecki for the kind hospitality at the University of Alberta.

Part of this work was carried out while AC and MŚ were visiting the Kavli Institute for Theoretical Physics in Santa Barbara, with partial support by the National Science Foundation under Grant No. PHY99-07949.

---

[1] I. Blokland, A. Czarnecki, M. Ślusarczyk, and F. Tkachov, Phys. Rev. Lett. **93**, 062001 (2004).
[2] A. Czarnecki and K. Melnikov, Phys. Rev. Lett. **78**, 3630 (1997).
[3] A. Czarnecki and K. Melnikov, Phys. Rev. **D59**, 014036 (1999).
[4] A. Czarnecki and K. Melnikov, Phys. Rev. Lett. **88**, 131801 (2002).
[5] A. Czarnecki and K. Melnikov, Nucl. Phys. **B505**, 65 (1997).
[6] J. Franzkowski and J. B. Tausk, Eur. Phys. J. **C5**, 517 (1998).
[7] For a review see, for example, F. V. Tkachov, Sov. J. Part. Nucl. **25**, 649 (1994) [arXiv:hep-ph/9701272].
[8] F. V. Tkachov, Phys. Lett. **B100**, 65 (1981).
[9] S. A. Larin, F. V. Tkachov, and J. A. M. Vermaseren, Phys. Lett. **B272**, 121 (1991).
[10] S. A. Larin, F. V. Tkachov, and J. A. M. Vermaseren, Phys. Rev. Lett. **66**, 862 (1991).
[11] D. J. Broadhurst, Z. Phys. **C54**, 599 (1992).
[12] T. van Ritbergen and R. G. Stuart, Phys. Rev. Lett. **82**, 488 (1999).
[13] T. van Ritbergen, Phys. Lett. **B454**, 353 (1999).
[14] S. Laporta, Int. J. Mod. Phys. **A15**, 5087 (2000).
[15] In common mathematical parlance this solution could be called "brute force". Since this does not do justice to the intellectual effort required for an efficient implementation of this approach, we use the word "targeted".
[16] J. A. M. Vermaseren, (2000), math-ph/0010025.
[17] Our computations are performed with the facilities of the Centre for Symbolic Computation at the University of Alberta.
[18] J. Fleischer and M. Yu. Kalmykov, Comput. Phys. Commun. **128**, 531 (2000), hep-ph/9907431. Some of the master integrals have incorrect signs for the imaginary terms, though; these errors are listed in the footnote on p.12 of hep-ph/0212319. We thank M. Kalmykov for his help with this issue.
[19] T. van Ritbergen and R. G. Stuart, Nucl. Phys. **B564**, 343 (2000).
[20] D. J. Broadhurst, N. Gray, and K. Schilcher, Z. Phys. **C52**, 111 (1991).
[21] J. A. M. Vermaseren, Int. J. Mod. Phys. **A14**, 2037 (1999).
[22] E. Remiddi and J. A. M. Vermaseren, Int. J. Mod. Phys. **A15**, 725 (2000).
[23] J. Blümlein, *Integrals in Diagram Calculations*, 2004 (unpublished).
[24] M. Jeżabek and J. H. Kühn, Nucl. Phys. **B314**, 1 (1989).
[25] M. Jeżabek and J. H. Kühn, Phys. Rev. **D48**, 1910 (1993), e: ibid. **D49**, 4970 (1994).
[26] A. Czarnecki and K. Melnikov, Nucl. Phys. **B544**, 520 (1999).
[27] K. G. Chetyrkin, R. Harlander, T. Seidensticker, and M. Steinhauser, Phys. Rev. **D60**, 114015 (1999).
[28] F.V.Tkachov, talk at CPP2001, hep-ph/0202033; http://www.inr.ac.ru/~ftkachov/projects/bear/.
[29] C. Anastasiou and A. Lazopoulos, JHEP **0407**, 046 (2004) [arXiv:hep-ph/0404258].